jove

High-Temperature and High-Pressure In situ Magic Angle Spinning Nuclear Magnetic Resonance Spectroscopy

Nicholas R. Jaegers[1], **Wenda Hu**[2], **Yong Wang**[1], **Jian Zhi Hu**[1]

[1] Pacific Northwest National Laboratory [2] Washington State University

Corresponding Author

Jian Zhi Hu

Jianzhi.Hu@pnnl.gov

Citation

Jaegers, N.R., Hu, W., Wang, Y., Hu, J.Z. High-Temperature and High-Pressure In situ Magic Angle Spinning Nuclear Magnetic Resonance Spectroscopy. *J. Vis. Exp.* (164), e61794, doi:10.3791/61794 (2020).

Date Published

October 9, 2020

DOI

10.3791/61794

URL

jove.com/video/61794

Abstract

Nuclear magnetic resonance (NMR) spectroscopy represents an important technique to understand the structure and bonding environments of molecules. There exists a drive to characterize materials under conditions relevant to the chemical process of interest. To address this, in situ high-temperature, high-pressure MAS NMR methods have been developed to enable the observation of chemical interactions over a range of pressures (vacuum to several hundred bar) and temperatures (well below 0 °C to 250 °C). Further, the chemical identity of the samples can be comprised of solids, liquids, and gases or mixtures of the three. The method incorporates all-zirconia NMR rotors (sample holder for MAS NMR) which can be sealed using a threaded cap to compress an O-ring. This rotor exhibits great chemical resistance, temperature compatibility, low NMR background, and can withstand high pressures. These combined factors enable it to be utilized in a wide range of system combinations, which in turn permit its use in diverse fields as carbon sequestration, catalysis, material science, geochemistry, and biology. The flexibility of this technique makes it an attractive option for scientists from numerous disciplines.

Introduction

Spectroscopic analysis of samples is an analytical tool used to gain valuable information about materials of interest such as their chemical state, structure, or reactivity. In a simplistic view, nuclear magnetic resonance (NMR) is one such technique that utilizes a strong magnetic field to manipulate the spin state of atomic nuclei to better understand the chemical environment of the species of interest. The nuclear spin state refers to the relative direction of the magnetic moment induced by the motion of the spinning nucleus, a

positively charged particle. In the absence of a magnetic field, the nuclear spins are randomly oriented but in the presence of a magnetic field, nuclear spins preferentially align with the external field of the magnet in a low energy spin state. This splitting of spin states to discrete energy values is known as the Zeeman effect. The difference between these energy levels (ΔE) is modeled by Equation 1:

$$\Delta E = h\gamma B_0 \qquad \text{Eq. 1}$$

where h is Plank's constant, B_0 is the strength of the external magnetic field and γ is the gyromagnetic ratio of the nucleus. The chemical environment of these spins also applies slight perturbations to these energy levels. Radio waves of corresponding frequencies can be used to excite the nuclei, which generates a transverse magnetization due to spins gaining phase coherence as longitudinal magnetization (based on the population of spins in parallel and anti-parallel states) is decreased. As the nuclei continue precessing about the axis of the magnetic field, the rotating magnetic movement creates a magnetic field that is also rotating and generating an electric field. This field modulates the electrons in the NMR detection coil, generating the NMR signal. Slight differences in the chemical environment of the nuclei in the sample affect the frequencies detected in the coil.

NMR analysis of solid samples introduces complexities not found in fluids. In fluids, the molecules tumble at fast rates, averaging the chemical environment spatially around the nuclei. In solid samples, no such averaging effect occurs, introducing an orientation-dependent chemical environment and broad spectral lines in the NMR signal. To mitigate these challenges, a technique known as magic angle spinning (MAS) is employed[1,2]. In MAS NMR, the samples are quickly rotated (several kilohertz) at an angle of 54.7356° with respect to the external magnetic field using an external spinning mechanism to address the orientation-dependent (anisotropic) interactions of NMR. This substantially narrows the NMR features and enhances the spectral resolution by averaging the orientation-dependent terms of the chemical shift anisotropy, dipolar interactions, and quadrupolar interactions. Two notable exceptions do hinder the line narrowing abilities of MAS NMR. The first is strong homonuclear coupling sometimes present in ^{1}H NMR that requires high spinning speeds (~70 kHz) to remove. However, the significantly elevated temperatures of the high temperature applications will greatly suppress the ^{1}H homonuclear interaction by imparting enhanced thermal motion such that a much reduced sample spinning rate can be utilized for significantly enhanced spectral resolution. Furthermore, with the technology continuously evolving, rotors with smaller diameters can now be fabricated to achieve spinning rates far exceeding 5 kHz, which helps to further suppress the ^{1}H homonuclear dipolar interactions. The second exception is residual second-order quadrupolar interactions for nuclei with spin that exceeds one-half since only the first order term is eliminated at the magic angle, leaving more complex lineshapes that can only be improved by stronger external magnetic fields. It should be emphasized that 2D MQMAS techniques can be readily incorporated into the current technology so that a true isotropic chemical shift spectrum can be obtained in a similar way as to the standard MQMAS experiments[3].

MAS NMR has enabled detailed characterization of solid materials, strengthening the quality of observations. However, the necessity of spinning the samples in NMR rotors (the sample holder) at high rates also imposes challenges in conducting experiments at elevated temperatures and pressures which may be more relevant to the conditions of interest. It may, at times, be desirable to examine materials under conditions that are relatively harsh for NMR rotors. A number of efforts have successfully adapted liquid-state NMR technologies to conduct high-temperature, high-pressure NMR[4,5,6,7]; however, commercial rotor caps used for solid-state MAS NMR may be expelled from the rotor at high pressures, causing significant damage to the equipment. Such effects may be compounded by examining a decomposition reaction that greatly increases the pressure in the sample holder. As such, new designs are required to effectively and safely conduct in situ NMR experiments. For example, the rotor must adhere to several qualities for effective use in MAS NMR, namely non-magnetic, lightweight, durable, temperature resistant, low NMR background material, sealable, high-strength, and chemical resistant. The pressures the rotor must withstand are quite large. Not only must the rotor withstand the pressure of the sample contained within (e.g., high-pressure gas), the rotation of the device imparts centrifugal force which has its own contribution to the total system pressure[8], P_T, by equation 2:

$$P_T = \frac{(R_O^2 - R_I^2) * \rho * \omega^2 * R_O}{2 * R_I} + P_S \qquad \text{Eq. 2}$$

R_I and R_O are the inner and outer rotor radii, respectively, ω is the rotational frequency in radians per second, and P_S is the sample pressure.

A number of strategies have been developed to address these concerns[9]. Early examples resembled flame-sealed tubes[10,11,12] or polymer inserts[13,14], which were insufficient for extended, fine-controlled operation at elevated temperatures and pressures. Iterations to rotor designs have suffered from limitations in the maximum operating temperature imparted by the use of epoxy or sample volume reductions from ceramic inserts[8,15,16]. A recent technology reduces unit production costs by employing simple snap-in features in a commercial rotor sleeve, but offers relatively less control over the conditions with which it can operate[17]. The design employed herein is an all-zirconia, cavern-style rotor sleeve milled with a threaded top[18]. A cap is also threaded to allow for a secure seal. Reverse threading prevents sample rotation from loosening the zirconia cap and an O-ring constitutes the sealing surfaces. This rotor design is visible in **Figure 1** and similar rotors and instructions to make them have been patented[19]. Such a strategy enables high mechanical strength, chemical resistance, and temperature tolerance.

These designs are suitable for temperatures and pressures of at least 250 °C and 100 bar, limited in temperature by readily-available NMR probe technology. When combined with specialized sample preparation equipment, it represents a truly powerful technique that has been employed for far-reaching applications as carbon sequestration, catalysis, energy storage, and biomedicine[20]. Such equipment includes a way to pretreat the solid materials to remove unwanted surface species such as water. A furnace is often employed for this step. A dry box is typically used to load the solid samples into the NMR rotor. From there, the rotor is transferred into an exposure device which enables the rotor to be opened under a tightly controlled atmosphere to load a

desired gas or mixture into the rotor. Such a device is depicted in **Figure 2**.

Protocol

The protocol is divided into four sections which specify 1) the preparation of any solid materials being used in the system or activation or clearing of undesired adsorbed species, 2) addition of the solid and liquid materials to the NMR rotor, 3) addition of gases to the rotor, and 4) conducting the NMR experiments in the spectrometer. The procedure is representative of a typical sequence but may be modified to fit the specific needs of the experiment.

1. Pretreating solid samples

1. Weigh approximately twice the mass of the solid sample that is desired for the NMR experiment (for a 7.5 mm rotor, ~250 mg) and place the solid sample into a quartz sample tube used for treating materials in a furnace system, plugging the tube with quartz wool to hold the material in place.
2. Connect the isolation valves to the solids treatment 1) flow or 2) vacuum system by placing the tube into the cool furnace and tightening the connections.
3. Affix the quartz tube end(s) onto the gas isolation valve(s) in the open position.
4. Begin the treatment.
    1. For flow systems:
        1. Affix a thermocouple to the outside of the tube, holding it in place with a heat-resistant material.
        2. Begin the flow of the treatment gas (e.g., N_2 at 100 sccm) to clear the solid surface or activate the material.
    2. Alternatively, for vacuum systems:
        1. Close the isolation valve to the vacuum system and start the vacuum pump.
        2. When full vacuum is established, very slowly open the isolation valve to apply vacuum to the sample, pausing periodically to allow the system to equilibrate. Continue until the valve is open.
5. Turn on the furnace controller and set the temperature ramp program to the desired condition (e.g., 300 °C for 4 hours at a ramp rate of 5 °C/min).
6. Start the temperature program and let it run.
7. When completed, allow the sample to cool to a workable temperature.
8. Turn off the temperature controller and stop the flow/ vacuum.
9. Quickly seal the sample with the isolation valves to maintain the desired sample environment.
10. Disconnect the quartz tube from the treatment system and transfer the tubes and closed valves to the antechamber of a dry, N_2-purged glove box.
11. Empty and refill the antechamber at least 4 times and transfer the tube inside of the glove box.

2. Loading solid samples into the NMR rotor

1. Weigh the empty and clean high-pressure, high-temperature NMR rotor with the rotor cap.
2. Place the NMR rotor in the holder to maintain directionality.
3. Place the sample funnel into the bore of the rotor.
4. Remove the isolation valve(s) from the sample tube and pour a small quantity of solid material into the funnel.

5. Tap the powder down into the funnel and lightly direct it into the rotor with the packing rod as necessary.
6. Repeat the stepwise addition of solid material until the desired quantity (e.g., ½ rotor) is achieved.
7. Weigh the NMR rotor (and cap) with the sample inside to determine the quantity of sample added.
8. If desired, draw up a specified quantity of any liquid sample and slowly inject the liquid into the center of the NMR rotor with a micro syringe.
9. Seal the rotor by placing the cap onto the top and turning it counterclockwise with the rotor cap bit to engage the O-ring between the rotor and cap. Note that a new O-ring may be periodically required to prevent leaking, especially if using chemically abrasive mixtures or small gases such as hydrogen.
10. Weigh the NMR rotor to determine the total mass of added sample.

3. Charging the NMR rotor with the desired chemicals at the desired conditions

1. Place the sealed NMR rotor into the rotor stage, ensuring the size of the stage insert is compatible with the rotor size, and tighten the nut by hand to secure it in place. Note that the tightness of the rotor in the holder in this step will determine the tightness of the cap seal.
2. Lower the rotor stage into the lower section of the high-pressure exposure device.
3. Use an Allen wrench to turn one of the screws 90° to secure the rotor stage into the bottom of the exposure device.
4. Place the top section of the NMR loading device into and on top of the bottom section, lining up the NMR cap bit to the top of the cap head of the NMR rotor to ensure it is engaged.
5. Place the 2 clamps over the top of the lip where the upper and lower sections of the exposure device meet and latch them in place.
6. Tighten the 6 bolts on the top of the upper section of the exposure device to engage the sealing surface between the upper and lower sections.
7. Connect the upper section of the NMR exposure device to the gas line inlet and outlets.
8. Connect the thermocouple on the upper section of the NMR exposure device to the temperature sensor.
9. If desired, wrap the heating tape around the gas lines and upper sections of the exposure device to enable heating with the respective controller. A hot plate can also be engaged.
10. Ensuring the exposure chamber outlet is open and source gas valve is closed, turn on the vacuum pump to remove air from the exposure device and associated lines.
11. Purge the lines with either the desired gas or an inert one, cycling between vacuum and atmospheric pressure three times to ensure the lines are cleared of air.
12. Prepare the desired gas composition either from 1) a high-pressure delivery system or 2) a flow system to introduce vapors at a specified pressure.
    1. For high-pressure or vacuum sample preparation:
        1. Close the exposure device gas outlet and set the gas manifold valves to bypass the liquid injection line.
        2. Set the desired pressure on the high-pressure syringe pump of the high-pressure delivery system.

3. Open the gas source valves on the high-pressure syringe pump and run the program set on the pump, monitoring the real pressure inside of the exposure device.
4. When the desired pressure is achieved inside the exposure device, stop the syringe pump and close the source gas valves.
5. Open the NMR rotor by rotating clockwise the external screw mechanism, which is coupled to the interior NMR cap bit.
6. Allow the gas of the desired pressure to enter the NMR rotor and equilibrate.
7. Reseal the NMR rotor by rotating the external screw mechanism counterclockwise. A viewing window will assist in determining when the rotor is closed.
8. Slowly depressurize the system by opening the exposure device gas outlet valve.

2. For flowing gas or vapor sample preparation:
    1. Ensure the exposure device gas outlet is open to prevent over-pressure.
    2. Set the desired gas flow rate on the mass flow controller and begin the gas flow.
    3. Connect the liquid supply line from the liquid syringe pump to the gas manifold.
    4. Set the gas manifold valves to enable flow to the liquid injection line.
    5. Set the liquid flow rate on the liquid syringe pump to achieve the desired vapor pressure and begin liquid injection.
    6. Open the NMR rotor by rotating clockwise the external screw mechanism which is coupled to the interior NMR cap bit.
    7. Allow the system to equilibrate to the desired gas pressures inside the NMR rotor and reseal the NMR rotor by rotating the external screw mechanism counterclockwise. A viewing window will assist in determining when the rotor is closed.
    8. Stop the liquid syringe pump injection and configure the valves to bypass the liquid injection line, disconnecting the pump from the system.
    9. Stop the flowing gas.
13. Purge the system with an inert gas to remove any potentially toxic or flammable gases.
14. Stop any heating and allow the system to cool.
15. Disconnect any heating tape and the thermocouple.
16. Disconnect the inlet and outlet gas lines.
17. Loosen the 6 bolts on the top of the exposure device to compromise the seal.
18. Unclip the 2 clamping sections and remove them from the exposure device.
19. Carefully lift the upper section up and off the lower section.
20. Use an Allen wrench to loosen the rotor stage and draw it up with the threaded rod.
21. Loosen the nut on the rotor stage and remove the rotor from the device component.
22. Weigh the rotor to ensure the desired gas quantities are present.

4. Conducting the MAS NMR experiment

1. Place the NMR rotor into the NMR coil on the NMR probe.

2. Raise the probe into the magnet bore and lock it into place.
3. Initiate sample spinning using the MAS control box and adjust to the desired rotor spinning rate.
4. Use the computer to begin the tuning/match sequence on the desired channel.
5. Adjust the tuning/match settings on the probe to optimize the probe electronics.
6. Exit the tuning/match sequence on the computer and set up the desired experimental parameters (e.g., pulse sequence, experiment array, temperature, etc.).
7. Collect the MAS NMR data.

Representative Results

The output from the NMR spectrometer takes the form of a free induction decay (FID) which is the time-domain signal from the excited spins as they relax back to thermodynamic equilibrium. Such an FID resembles **Figure 3**. When Fourier transformed from the time domain to the frequency domain (frequency to PPM by Equation 3, whereby the difference absolute frequency and a reference is divided by the carrier frequency of the NMR spectrometer), it represents the NMR spectrum for which each peak indicates a nucleus in a unique chemical environment (**Figure 3**).

$$PPM = \frac{f - f_{ref}}{SF} * 10^6 \qquad \text{Eq. 3}$$

One representative result from an in situ high-temperature, high-pressure MAS NMR experiment comes from the field of catalysis[21]. In this investigation, the reaction pathways for the conversion of ethanol to butenes were explored to elucidate the mechanism for biogenic molecules upgrading to jet fuel. This reaction takes place at elevated pressure and temperature, necessitating in situ NMR experiments conducted at 210 °C and 100 psig. In the cascade of reactions, ethanol is converted to crotonaldehyde through acetaldehyde and acetaldol. It has been shown that Meerwein–Ponndorf-Verley reduction to crotyl alcohol may be a step in the further conversion of crotonaldehyde, but the specific steps to form butenes after crotonaldehyde formation are poorly understood. To investigate this, time-resolved ^{1}H NMR at 300 MHz was employed to monitor the conversion of ethanol (and crotonaldehyde) to butene products. A portion of the pertinent data can be found in **Figure 4**. Approximately 25 mg of 4% Ag/4% ZrO_2/SiO_2 was placed into the NMR rotor along with the liquid component of the feed to generate a wet solid sample. The rotor atmosphere was charged with H_2 (a reactant with a broad resonance at 4.35 ppm) to bring the total pressure at reaction temperature to 100 psig.

^{1}H NMR spectra were collected every 64 seconds to monitor the transitions of the chemical species present as the temperature was increased to 210 °C. From the onset of crotonaldehyde conversion, resonance features characteristic of crotonaldehyde (9.4, 7.05, and 6.12 ppm, black dotted line) are suppressed as these molecules convert to product and intermediate species overtime. Crotonaldehyde exhibits a transient adsorbed-like species (9.28, 6.3, and 5.8 ppm, blue dotted line) at lower temperatures, which dissipates as a feature characteristic of butyraldehyde develops at 9.7 ppm (red dotted line). Butyraldehyde signal intensity initially intensifies, reaching a maximum at about 800 s before it begins to dissipate. Concomitant with its consumption, peaks consistent with 1-butene and 2-butene at 5.65 and 5.3 ppm (green dotted line) arise and grow with time. Also apparent from the NMR spectra is the temperature-dependent chemical shift of butyraldehyde and crotonaldehyde, which shift higher as the temperature is elevated, indicative of thermal perturbation to the shielding

of the proton nuclei in these polar molecules and potentially indicating vaporization at elevated temperatures[22].

This series of spectra provides some insight into the operational reaction mechanism for the conversion of ethanol to butenes. The consumption of butyraldehyde, coupled with the simultaneous appearance of peaks characteristic of n-butenes, suggests that butyraldehyde is an intermediate in the formation of n-butene. Additional in situ high-temperature, high-pressure MAS NMR experiments have highlighted the role of surface hydrogen species, the role of ethanol protons, adsorbed olefins, and further insight into the system[23]. Further, the low-field region (not shown) offers additional transient information which compliments the results shown in **Figure 4** which helps affirm the peak identification and supplements the observations already noted. The wealth of information extracted for just this system highlights some of the capabilities possible with in situ NMR.

In addition to applications in catalysis, in situ, high-temperature, high-pressure MAS NMR can be used to better understand the evolution of chemical species for biological applications. For example, the thermal degradation of liquids used in electronic cigarettes is of great concern to the health and well-being of users since toxic compounds may be generated and subsequently inhaled. Due to the variety of species present in such systems, ^{13}C MAS NMR exhibited beneficial signal resolution for the assignment of spectral features, leading to a discernment of the pathways for thermochemical transformation. The results showed that at temperatures between 130 and 175 °C, the principal components of vape juices would degrade via an oxidative, radical-mediated mechanism. A representative ^{13}C MAS NMR spectrum is depicted in **Figure 5**. In this, parent glycerol is shown to be present at 63 and 73 ppm (with spinning sidebands, *). As time progresses at 130 °C in an O_2 environment, new features emerge across the spectral range. Key features indicative of toxins are highlighted by their chemical structures. Namely, acrylic acid and formic acid/formaldehyde are observed to form at 175 and 164 ppm, respectively. Further, oxidation product CO_2 is observed at 125 ppm. Most importantly, even at such low temperatures, acetal-species of formaldehyde and acetaldehyde are shown to form between 50 and 112 ppm. The addition of parent glycerol to formaldehyde and acetaldehyde generates new hemiacetal species which act as aldehyde carriers. These can self-interact and dehydrate to generate new acetal species as well. Distinct peaks at 105 and 112 ppm correspond to acetaldehyde-derived acetals. Numerous other peaks between 50 and 80 ppm correspond to the many other chemical environments of the hemiacetals and acetals. Such observations enable the identification of toxic compounds which may be inhaled under conditions relevant to electronic cigarette use, highlighting the flexibility of the MAS NMR method in addressing problems across many disciplines.

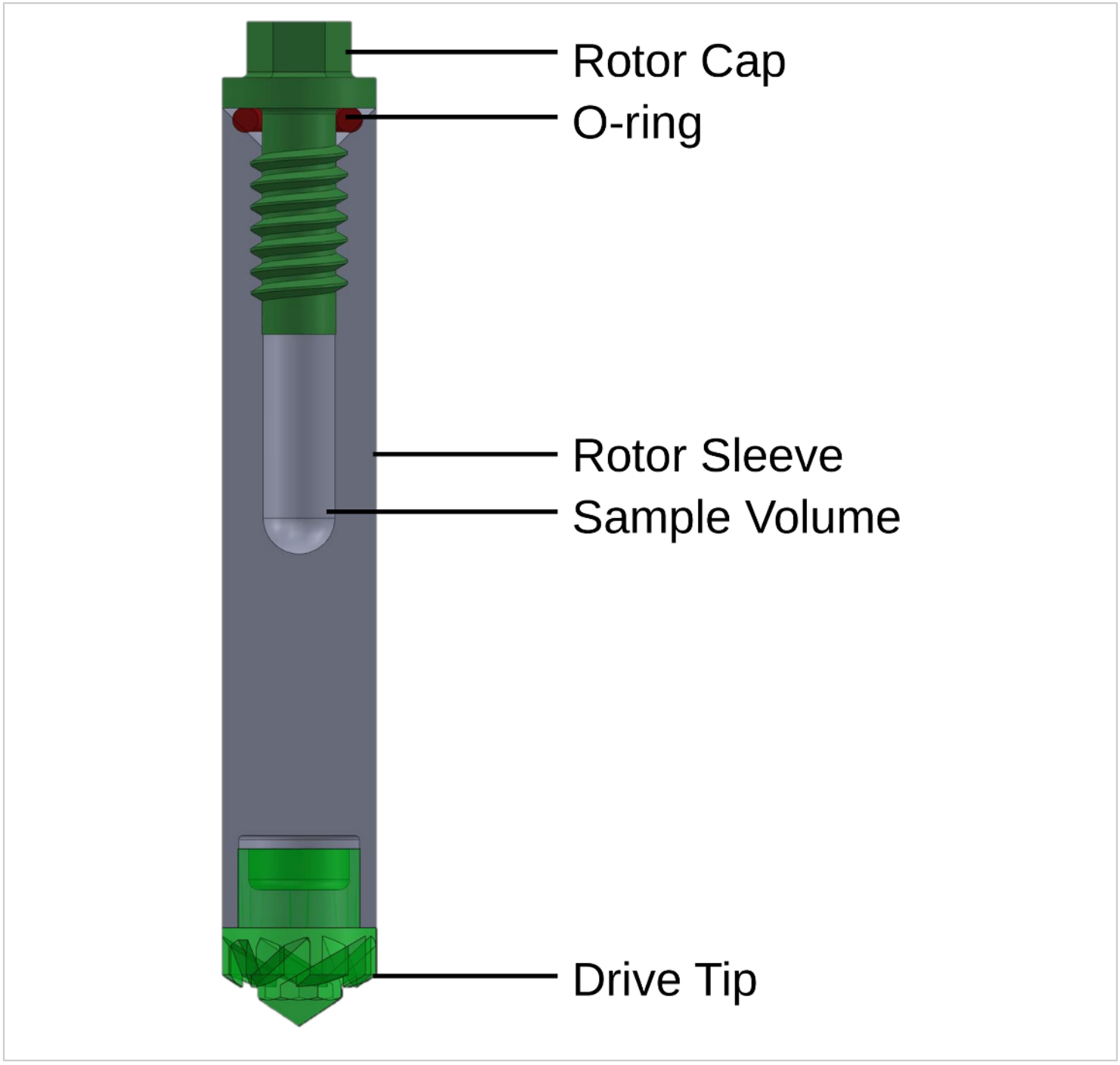

Figure 1: Cross-section diagram of the high-temperature, high-pressure MAS NMR rotor. The rotor consists of four main components. The cylindrical rotor sleeve is the main body of the sample holder. It contains a caver for the samples space and threads at the top. The rotor cap screws into the sleeve threads where it compresses an O-ring, making the seal. An NMR drive tip is fitted into the bottom of the rotor sleeve to enable spinning in the NMR spectrometer. Adapted with

permission from reference 20. Copyright 2020 American Chemical Society. Please click here to view a larger version of this figure.

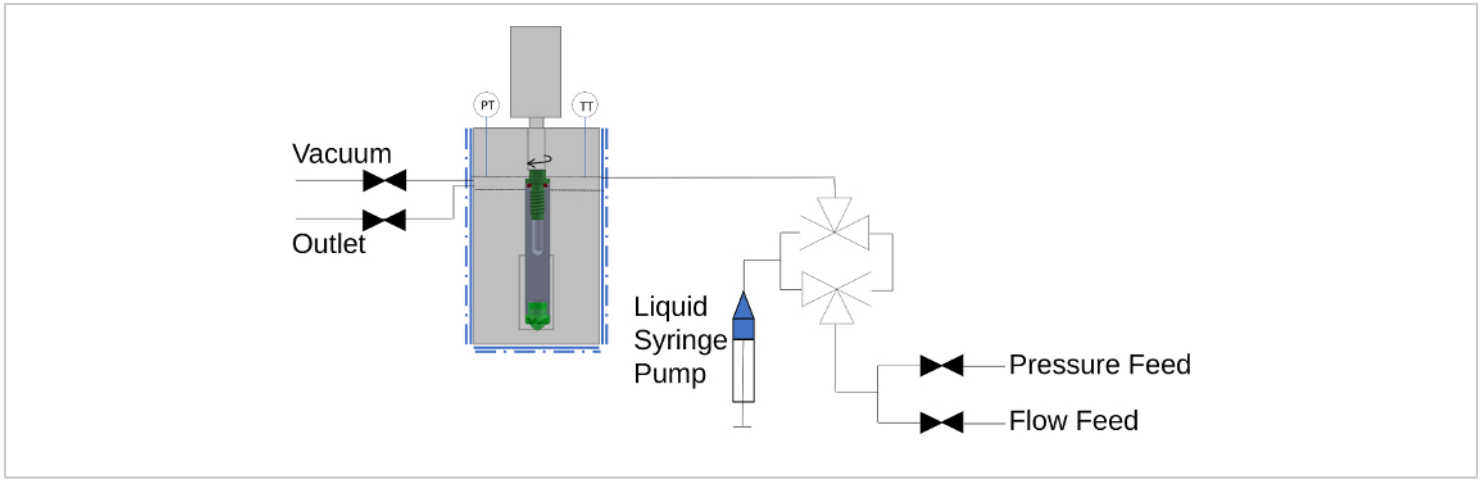

Figure 2: Schematic diagram of the high-temperature, high-pressure NMR exposure device chamber. The NMR rotor is placed within the high-temperature, high-pressure exposure device, affixed in the stage. Pressure and temperature gauges monitor the condition inside the chamber. Gas lines are connected to the loading chamber which connect to a vacuum supply, outlet discharge, and gas feeds. The gas feed connects to a high-pressure syringe pump supply as well as a gas flow manifold. An optional liquid feed line can be selected in flow mode via two three-way valves. The rotor can be opened and closed in the controlled environment using a rotating mechanism coupled with the inside screw bit engaged onto the NMR cap. Adapted with permission from reference 20. Copyright 2020 American Chemical Society. Please click here to view a larger version of this figure.

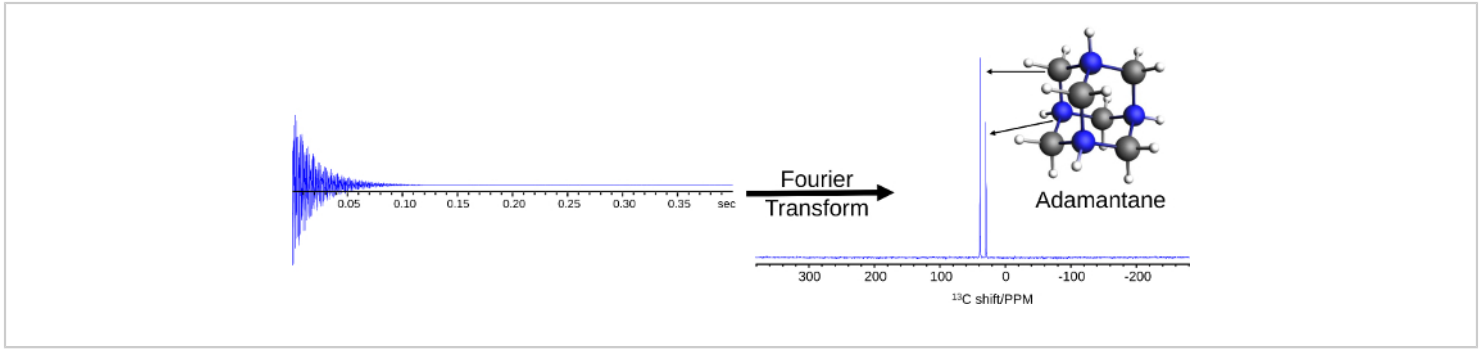

Figure 3: Representative FID and spectrum from an NMR experiment. The ^{13}C NMR result illustrates the Fourier transform of the FID to the NMR spectrum. The ^{13}C NMR spectrum identifies two distinct chemical environments, representative of the two types of carbon atoms in adamantane at 38.48 ppm (grey carbon) and 29.39 ppm (blue carbons). Please click here to view a larger version of this figure.

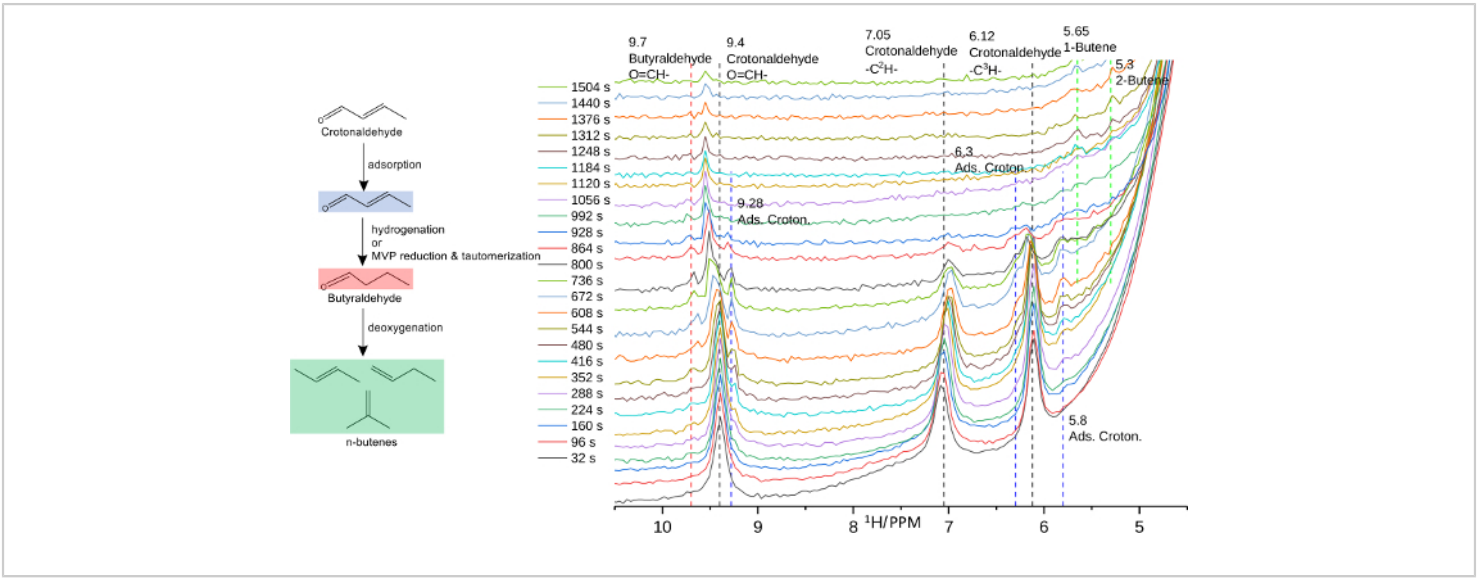

Figure 4: In situ ^{1}H MAS NMR time sequence of ethanol to butadiene on $Ag/ZrO_2/SiO_2$ catalysts under H_2 pressure. The left side summarizes the observed NMR phenomena. Peaks corresponding to crotonaldehyde at 9.4, 7.05, and 6.12 ppm dissipate as peaks at 9.28, 6.3, and 5.8 ppm develop, which are assigned to an adsorbed crotonaldehyde species. Subsequently, the signature peak of butyraldehyde at 9.7 ppm is observed and then dissipates as butenes appear at 5.65 and 5.3 ppm. Please click here to view a larger version of this figure.

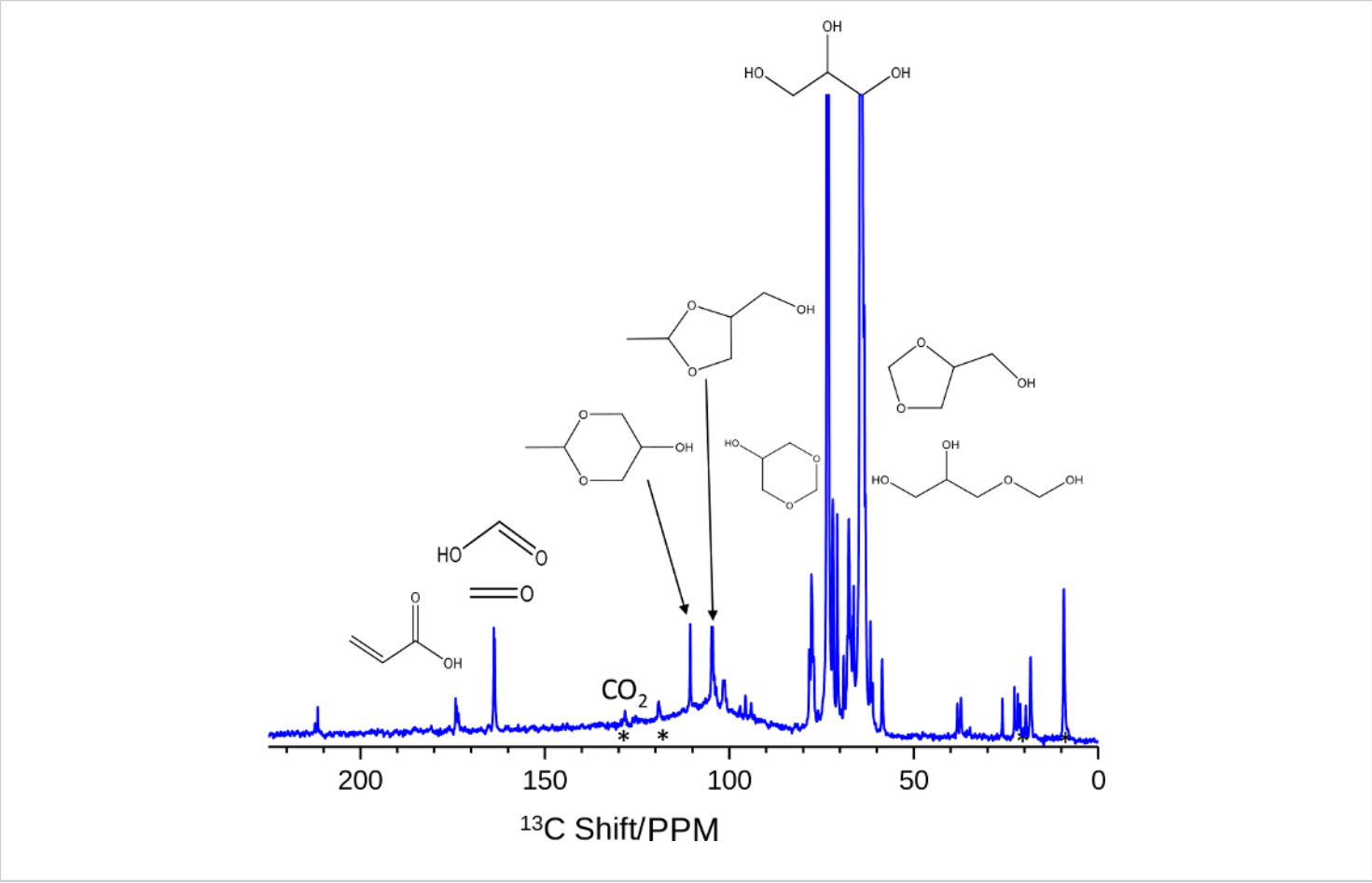

Figure 5: In situ ^{13}C MAS NMR data for the oxidative thermal decomposition of glycerol. A representative single-pulse ^{13}C MAS NMR spectrum acquired at 3.5 kHz for the oxidative (75 psig O_2) degradation of glycerol (63 and 73 ppm). At extended times at 130°C, new features assigned to acrylic acid and formic acid/formaldehyde are observed to form at 175 and 164 ppm, respectively. CO_2 is also observed at 125 ppm. Hemiacetals and acetal species from the combination of glycerol to formaldehyde and acetaldehyde are also apparent by the array of signals between 50 and 112 ppm. Typical spectral parameters included a π/4 pulse width, 400 ms acquisition time, and a 4 s recycle delay over a few thousand repetitions. ^{1}H decoupling was active. Please click here to view a larger version of this figure.

Discussion

The method of conducting MAS NMR spectroscopic measurements outlined herein represents the state of the art for conducting high-temperature, high-pressure MAS NMR. Such methods enable the observation of interactions occurring in vacuum atmospheres up to several hundred bar and from low temperatures (well below 0 °C to 250 °C) in a reliable, reproducible fashion. The ability to probe systems containing mixtures of solids, liquids, and gases under flexible chemical environments enables a wide range of experiments for diverse interests.

While many of the previous efforts have centered around the utilization of relatively large (7.5 mm) NMR rotors at low

magnetic fields (300 MHz), the nature of the design makes it scalable to smaller rotor sizes for faster spinning at higher magnetic fields. The extension of operation to such smaller sizes enables a wider array of nuclei to be probed. While ^{1}H and ^{13}C are standard at 300 MHz, in situ ^{27}Al MAS NMR, for example, greatly benefits from faster spinning rates and higher magnetic fields. In situ high-temperature, high-pressure NMR rotors as small as 3.2 mm are currently in operation for detection at spinning rates up to 25 kHz. The use of even smaller rotors (2.5 mm and 1.6 mm) would facilitate even faster spinning rates up to 35 or 45 kHz, respectively, which would be especially beneficial for quadrupolar nuclei. As the rotor sizes become smaller, the challenges to seal, spin, and handle the rotors all become greater. It should also be noted that the rotors described herein were designed to operate in probes compatible with Varian NMR systems, but these same principles could drive the development of similar rotors compatible with Bruker systems, taking care to adhere to physical dimensions of the rotor as well as the tight sealing which would be required of a cap located below the sample. Achieving such feats would extend the potential applications of the method even further.

While flexible, the application of this method is limited by several attributes. Chief among these limitations is the resource requirements to operate the NMR instrument in under conditions of high temperature and pressure. The specialized loading chamber and all-zirconia rotors are custom devices which are not readily available nor easily fabricated; however, an alternate high-temperature, high-pressure design[17], which offers less flexibility given the nature of plastic snap-in bushings and a minimum operating pressure exceeding ambient, is commercially available in 5 mm and 7.5 mm rotor diameters. Another limitation is that, while the pressure range is quite large (vacuum to more than 100 bar), the temperature range is limited to around 250 °C by commercially available NMR probes. Current efforts are underway to expand this range by the design of novel NMR probes. Indeed, one such effort has resulted in MAS NMR data acquisition at 325 °C and 60 bar[24]. Many reactions in catalysis require even higher temperatures, limiting what can be studied by the technique. Further, spinning at such temperatures can sometimes create instabilities in the rotation of the sample, causing the potential for a rotor crash. At temperatures substantially lower than 0 °C, rotor spinning is also complicated by the contraction of the plastic spin tip, which may unseat and crash the rotor as well. Spinning challenges such as these are quite common for mixtures of solids and liquids, which result in a sample with the consistency of a slurry. When such a sample is prepared, it is easy to distribute the weight heterogeneously within the rotor volume, which causes great difficulty in spinning due to notable weight imbalances and imparts resistance to rapid rotation. In practice, we have found it useful to, when possible, load the solid sample alone and spin it at rates comparable to the MAS NMR experiment. This takes advantage of the centrifugal force to evenly spread the solid material. The rotor can then be removed from the magnet, reopened in an inert environment, and the liquid can be slowly injected into the bottom of the central axis to promote an even weight distribution. Once the sample successfully spins, the chemical constituents will naturally approach an equilibrium distribution over time. Finally, another important limitation to this method is the requirement that the system operate in a batch reactor-type of mode. There is a strong drive to have flowing cells to mimic the conditions of fixed-bed reactors, however the successful implementation of such a system that enables spinning, minimizes leaking, and prevents channeling is of great difficulty. Some efforts have been made on this front

to varying degrees of success[25,26,27]. To do so at high pressures and temperatures brings further challenges to the endeavor.

Such NMR methods are adaptable to a variety of experimental conditions, making it an attractive technique for a diverse array of scientific disciplines. In addition to applications in catalysis, previous use has spanned across numerous fields. For example, in geochemistry in situ MAS NMR has been employed to better understand the complex speciation of aluminate species under highly alkaline environments to elucidate the chemistry in radioactive high-level waste[28,29,30]. The method has also been used in energy storage investigations to help identify the interactions between electrolytes components and electrode surfaces using in situ MAS NMR[31,32]. For biological applications, intact biological tissues have been analyzed to understand the chemical constituents at elevated temperatures without the concern of biofluid leaking[18]. The applications for which this technique can provide information are truly massive and expanding, highlighting the potential for widespread future use of in situ, high-temperature, high-pressure MAS NMR.

Disclosures

The authors declare the following competing financial interests. J.Z.H and colleagues hold a patent on the rotor design (US9151813B2). J.Z.H., N.R.J., et al. have filed a provisional patent application on the exposure device.

Acknowledgments

The review of catalyst applications was supported by the U.S. Department of Energy, Office of Science, Office of Basic Energy Sciences, Division of Chemical Sciences, Biosciences, and Geosciences Catalysis Program under contract DE-AC05-RL01830 and FWP-47319. The review of biomedical applications was supported by the National Institute of Health, National Institute of Environmental Health Sciences under grant R21ES029778. Experiments were conducted at EMSL (grid.436923.9), a DOE Office of Science User Facility sponsored by the Office of Biological and Environmental Research and located at Pacific Northwest National Laboratory (PNNL). PNNL is a multi-program national laboratory operated by Battelle for the U.S. Department of Energy under contract DE-AC05-RL01830 and FWP-47319.

References

1. Andrew, E. R., Bradbury, A., Eades, R. G. Nuclear Magnetic Resonance Spectra from a Crystal rotated at High Speed. *Nature.* **182** (4650), 1659-1659 (1958).
2. Lowe, I. J. Free Induction Decays of Rotating Solids. *Physical Review Letters.* **2** (7), 285-287 (1959).
3. Frydman, L., Fundamentals of Multiple-Quantum Magic-Angle Spinning NMR on Half-Integer Quadrupolar Nuclei. In *Encyclopedia of Nuclear Magnetic Resonance*, Grant, D. M., Harris, R. K., Eds. **9**, 262-274 (2002).
4. Khodov, I., Dyshin, A., Efimov, S., Ivlev, D., Kiselev, M. High-pressure NMR spectroscopy in studies of the conformational composition of small molecules in supercritical carbon dioxide. *Journal of Molecular Liquids.* **309** (2020).
5. Kolbe, F. et al. High-Pressure in situ 129Xe NMR Spectroscopy: Insights into Switching Mechanisms of Flexible Metal–Organic Frameworks Isoreticular to DUT-49. *Chemistry of Materials.* **31** (16), 6193-6201 (2019).
6. Ochoa, G. et al. (2) H and (139) La NMR Spectroscopy in Aqueous Solutions at Geochemical Pressures.

Angewandte Chemie International Edition. **54** (51), 15444-15447 (2015).

7. Hoffmann, H. C. et al. High-pressure in situ 129Xe NMR spectroscopy and computer simulations of breathing transitions in the metal-organic framework Ni2(2,6-ndc)2(dabco) (DUT-8(Ni)). *Journal of the American Chemical Society.* **133** (22), 8681-8690 (2011).
8. Turcu, R. V. F. et al. Rotor design for high pressure magic angle spinning nuclear magnetic resonance. *Journal of Magnetic Resonance.* **226**, 64-69 (2013).
9. Jaegers, N. R., Hu, M. Y., Hoyt, D. W., Wang, Y., Hu, J. Z., Development and Application of In situ High-Temperature, High-Pressure Magic Angle Spinning NMR. In *Modern Magnetic Resonance.* 1-19 (2017).
10. Miyoshi, T., Takegoshi, K., Terao, T. 13C High-Pressure CPMAS NMR Characterization of the Molecular Motion of Polystyrene Plasticized by CO2 Gas. *Macromolecules.* **30** (21), 6582-6585 (1997).
11. Miyoshi, T., Takegoshi, K., Terao, T. 129Xe n.m.r. study of free volume and phase separation of the polystyrene/poly(vinyl methyl ether) blend. *Polymer.* **38** (21), 5475-5480 (1997).
12. Miyoshi, T., Takegoshi, K., Terao, T. Effects of Xe Gas on Segmental Motion in a Polymer Blend As Studied by 13C and 129Xe High-Pressure MAS NMR. *Macromolecules.* **35** (1), 151-154 (2002).
13. Yonker, C. R., Linehan, J. C. The use of supercritical fluids as solvents for NMR spectroscopy. *Progress in Nuclear Magnetic Resonance Spectroscopy.* **47** (1), 95-109 (2005).
14. Deuchande, T., Breton, O., Haedelt, J., Hughes, E. Design and performance of a high pressure insert for use in a standard magic angle spinning NMR probe. *Journal of Magnetic Resonance.* **183** (2), 178-182 (2006).
15. Hoyt, D. W. et al. High-pressure magic angle spinning nuclear magnetic resonance. *Journal of Magnetic Resonance.* **212** (2), 378-385 (2011).
16. Vjunov, A. et al. Following Solid-Acid-Catalyzed Reactions by MAS NMR Spectroscopy in Liquid Phase-Zeolite-Catalyzed Conversion of Cyclohexanol in Water. *Angewandte Chemie International Edition.* **53** (2), 479-482 (2014).
17. Chamas, A. et al. High temperature/pressure MAS-NMR for the study of dynamic processes in mixed phase systems. *Magnetic Resonance Imaging.* **56**, 37-44 (2019).
18. Hu, J. Z. et al. Sealed rotors for in situ high temperature high pressure MAS NMR. *ChemComm.* **51** (70), 13458-13461 (2015).
19. Hu, J. Z., Hu, M. Y., Townsend, M. R., Lercher, J. A., Peden, C. H. High-pressure, high-temperature magic angle spinning nuclear magnetic resonance devices and processes for making and using same. *US patent.* (US9151813B2). (2015).
20. Jaegers, N. R., Mueller, K. T., Wang, Y., Hu, J. Z. Variable Temperature and Pressure Operando MAS NMR for Catalysis Science and Related Materials. *Accounts of Chemical Research.* **53** (3), 611-619 (2020).
21. Dagle, V. et al. Single-step Conversion of Ethanol to n-butenes over Ag-ZrO_2/SiO_2 catalysts. *ACS Catalysis.* **10** (18), 10602-10613 (2020).
22. Jaegers, N. R., Wang, Y., Hu, J. Z. Thermal perturbation of NMR properties in small polar and non-polar molecules. *Scientific Reports UK.* **10** (1), 6097 (2020).

23. Jaegers, N. R. Applications of In situ Magnetic Resonance Spectroscopy for Structural Analysis of Oxide-supported Catalysts. *Washington State University, dissertation.* (2019).
24. Mehta, H. S. et al. A novel high-temperature MAS probe with optimized temperature gradient across sample rotor for in-situ monitoring of high-temperature high-pressure chemical reactions. *Solid State Nuclear Magnetic Resonance.* **102**, 31-35 (2019).
25. Hu, J. Z. et al. A large sample volume magic angle spinning nuclear magnetic resonance probe for in situ investigations with constant flow of reactants. *Physical Chemistry Chemical Physics.* **14** (7), 2137-2143 (2012).
26. Jiang, Y. et al. In situ MAS NMR–UV/Vis investigation of H-SAPO-34 catalysts partially coked in the methanol-to-olefin conversion under continuous-flow conditions and of their regeneration. *Microporous and Mesoporous Materials.* **105** (1-2), 132-139 (2007).
27. Xu, S., Zhang, W., Liu, X., Han, X., Bao, X. Enhanced In situ Continuous-Flow MAS NMR for Reaction Kinetics in the Nanocages. *Journal of the American Chemical Society.* **131** (38), 13722-13727 (2009).
28. Graham, T. R. et al. In situ Al-27 NMR Spectroscopy of Aluminate in Sodium Hydroxide Solutions above and below Saturation with Respect to Gibbsite. *Inorganic Chemistry.* **57** (19), 11864-11873 (2018).
29. Zhang, X. et al. Boehmite and Gibbsite Nanoplates for the Synthesis of Advanced Alumina Products. *ACS Applied Nano Materials.* **1** (12), 7115-7128 (2018).
30. Zhang, X. et al. Transformation of Gibbsite to Boehmite in Caustic Aqueous Solution at Hydrothermal Conditions. *Crystal Growth & Design.* **19** (10), 5557-5567 (2019).
31. Hu, J. Z., Jaegers, N. R., Hu, M. Y., Mueller, K. T. In situ and ex situ NMR for battery research. *Journal of Physics: Condensed Matter.* **30** (46) (2018).
32. Hu, J. Z. et al. Adsorption and Thermal Decomposition of Electrolytes on Nanometer Magnesium Oxide: An in situ C-13 MAS NMR Study. *ACS Applied Materials & Interfaces.* **11** (42), 38689-38696 (2019).